

Article

# Quasi-Static and Low-Velocity Impact Behavior of Intraply Hybrid Flax/Basalt Composites

Fabrizio Sarasini <sup>1,\*</sup>, Jacopo Tirillò <sup>1</sup>, Luca Ferrante <sup>1</sup>, Claudia Sergi <sup>1</sup>, Pietro Russo <sup>2</sup>,  
Giorgio Simeoli <sup>2</sup>, Francesca Cimino <sup>2</sup>, Maria Rosaria Ricciardi <sup>3</sup> and Vincenza Antonucci <sup>3</sup>

<sup>1</sup> Department of Chemical Engineering Materials Environment, Sapienza-Università di Roma and UdR INSTM, Via Eudossiana 18, 00184 Roma, Italy; jacopo.tirillo@uniroma1.it (J.T.); luca.ferrante@uniroma1.it (L.F.); claudia.sergi@uniroma1.it (C.S.)

<sup>2</sup> Institute for Polymers, Composites and Biomaterials, National Research of Council, Via Campi Flegrei 34, 80078 Pozzuoli (NA), Italy; pietro.russo@unina.it (P.R.); giorgio.simeoli@unina.it (G.S.); francesca.cimino@ipcb.cnr.it (F.C.)

<sup>3</sup> Institute for Polymer, Composites and Biomaterials, National Research Council, Piazzale Enrico Fermi, 1, 80055 Portici (NA), Italy; mariarosaria.ricciardi@unina.it (M.R.R.); vinanton@unina.it (V.A.)

\* Correspondence: fabrizio.sarasini@uniroma1.it; Tel.: +39-0644585408

Received: 20 February 2019; Accepted: 19 March 2019; Published: 22 March 2019



**Abstract:** In an attempt to increase the low-velocity impact response of natural fiber composites, a new hybrid intraply woven fabric based on flax and basalt fibers has been used to manufacture laminates with both thermoplastic and thermoset matrices. The matrix type (epoxy or polypropylene (PP) with or without a maleated coupling agent) significantly affected the absorbed energy and the damage mechanisms. The absorbed energy at perforation for PP-based composites was 90% and 50% higher than that of epoxy and compatibilized PP composites, respectively. The hybrid fiber architecture counteracted the influence of low transverse strength of flax fibers on impact response, irrespective of the matrix type. In thermoplastic laminates, the matrix plasticization delayed the onset of major damage during impact and allowed a better balance of quasi-static properties, energy absorption, peak force, and perforation energy compared to epoxy-based composites.

**Keywords:** flax fibers; basalt fibers; intraply flax/basalt hybrid; low-velocity impact; mechanical properties

## 1. Introduction

The need to increase the mechanical performance of natural fiber composites to meet the requirements of at least semi-structural applications has triggered a resurgent interest in hybrid composites [1,2]. Indeed, fiber hybridization offers a comprehensive set of possibilities leading to synergetic effects or to properties not exhibited by the single constituents [3]. This approach has been successfully exploited in the field of low-velocity impact resistance of composite laminates [4], with the first studies aimed at increasing the damage tolerance of carbon fiber composites by adding more ductile fibers, mainly glass [5–7] and aramid [8–12]. Recently new fiber combinations have been investigated, mainly based on natural and synthetic fibers. Not only glass fibers [13,14] but also carbon fibers [15,16] have been successfully hybridized with natural fibers to enhance poor mechanical properties and moisture resistance of natural fiber composites.

Among the different combinations available, the use of flax fibers with natural fibers of mineral origin, such as basalt fibers [17], has been widely investigated in literature with promising results. Fragassa et al. [18] addressed the impact behavior of hybrid laminates made of basalt and flax fibers in a vinyl ester matrix. These hybrid laminates were manufactured using a sandwich-like configuration

with softer flax fibers in the core layers and the stronger basalt ones in the skins, in accordance with a stacking sequence typically used in impact resistant hybrid laminates [19].

Aside from intermediate tensile and flexural properties between those of basalt and flax fiber laminates, hybrid laminates showed a higher penetration energy compared to pure flax fiber composites. Recently Papa et al. [20] investigated the impact response of hybrid basalt/flax epoxy composites with an intercalated stacking sequence ([B,F]<sub>8s</sub>). Hybridization led to better impact performance compared to pure basalt and flax composites in terms of peak force and penetration energy along with a much lower delaminated area. This behavior was due, according to the authors, to the energy absorption ability of flax layers through a non-elastic mode and to the deflection of the impact damage progression. From the above-mentioned studies, it is evident that material dispersion can be considered as one of the most important parameters in hybridization under low-velocity impact loading [1].

In particular, it is important to differentiate the intraply hybridization, where yarns (tows) of two different fibers are mixed in the same ply, from the interply one, where plies of two homogeneous reinforcements are stacked. It is expected that intraply hybrid composites exhibit better resistance to crack propagation during an impact event, even though results in the literature are contrasting [21,22].

Compared to interply hybrid composites, which have been widely investigated in literature, intraply hybrid composites have received limited attention. Zhang et al. [23] studied the effects of different hybrid structures based on interlayer and intralayer warp-knitted fabrics with carbon and glass fibers under low-velocity impact conditions. Compared to the interlayer configuration, the intralayer hybrid showed a higher peak load and a smaller damage area at the same hybrid ratio and level of impact energy, thus, suggesting that a better impact resistance can be obtained by intralayer hybrid structures. Bandaru et al. [24] addressed the low-velocity impact response of 3D angle-interlock polypropylene composites reinforced with Kevlar and basalt fibers, and the intraply configuration was found to absorb more energy (7.67–48.49%) than the pure 3D Kevlar and basalt composites. Wang et al. [22] manufactured three-dimensional interply and intraply basalt–Kevlar/epoxy hybrid composites. The low-velocity impact test results demonstrated higher ductility indices, lower peak load, and higher specific energy absorption in both warp and weft directions of the interply hybrid composite compared to those of the intraply hybrid composite. In addition to the material dispersion, the impact behavior of a composite material is also significantly affected by matrix type and its toughness. Thermoplastic matrices are usually preferred over thermoset ones when an improvement in impact resistance and damage tolerance is required [25,26].

In this work, an intraply technology is presented, and this could represent an interesting solution for introducing flax fibers in at least semi-structural components. This work aims to evaluate the effect of two different matrices, namely a thermoset (epoxy) and a thermoplastic (polypropylene), on the mechanical properties of a new hybrid composite based on a commercially available hybrid woven fabric with basalt and flax fibers. The hybrid composites have been subjected to quasi-static flexural tests along with low-velocity impacts to investigate their mechanical behavior and correlate the resulting failure modes. To the best of authors' knowledge, no similar works are available combining, in a single study, this specific intraply hybridization with different polymer matrices.

## 2. Materials and Methods

### 2.1. Materials

LINCORE<sup>®</sup> HF T2 360 (Figure 1), provided by Depestele (Bourguebus, France), was a balanced Twill 2/2 woven fabric with an areal density of 360 g·m<sup>-2</sup> (50 wt% flax/50 wt% basalt; threads per cm in warp/weft = 3.6). Twill fabrics are common in the composite industry as they show longer thread flotation compared to plain woven fabrics and a lower level of fiber crimp, potentially leading to better mechanical properties and higher fiber packing density along with a better ability to conform to complex contours.



**Figure 1.** Close-up view of the dry flax/basalt hybrid fabric (dark yarn = basalt; bright yarn = flax).

The thermoset matrix was based on a two-component commercial epoxy system PRIME™ 20LV (100:26 resin/hardener weight ratio) supplied by Gurit (Newport, UK). The thermoplastic matrix was a polypropylene (PP, Bormod HF955MO) with a MFI@230 °C, 2.16 kg equal to 20 g/10 min. To increase the interfacial adhesion with both reinforcements, a PP-g-MA (maleic anhydride grafted polypropylene) coupling agent (2 wt%) from Chemtura (Philadelphia, USA) was used, namely Polybond 3000 (MFI@190 °C, 2.16 kg: 405 g/10 min; maleic anhydride content of 1.2 wt%). Polyolefins, such as polyethylene and polypropylene are known to exhibit a poor adhesion with natural fibers due to their hydrophobic long aliphatic primary chain without any polar groups. PP-g-MA coupling agent was chosen to react with the hydroxyl groups on the surface of both basalt and flax fibers [27,28].

The commercial polypropylene (PP) was modified with a coupling agent (PPc) by a co-rotating twin screw extruder Collin Teach-Line ZK25T with the following temperature profile: 180–190–205–195–185 °C from the hopper to the die, and with a screw speed of 60 rpm. Films of neat or compatibilized polypropylene with 2 wt% of coupling agent, with a thickness equal to 35–40 µm, were obtained by using a film blowing extrusion line model Teach-Line E 20 T from Collin GmbH (Maitenbeth, Germany) equipped with a calender CR72T (Maitenbeth, Germany). The processing was performed in accordance with the following temperature profile along the screw: 180–190–200–190–185 °C and a screw speed of 55 rpm.

## 2.2. Composite Materials Manufacturing

Thermoset-based laminates have been manufactured by vacuum infusion process by stacking 4 layers (0/90) of the hybrid fabric that were cured for 16 h at 50 °C as per manufacturer's specifications. Thermoplastic laminates were manufactured by alternating layers of polypropylene films (with or without coupling agent) and 4 hybrid fabrics by the film-stacking technique using a compression molding machine (model P400E, Collin GmbH, Maitenbeth, Germany) in accordance with the pre-optimized molding cycle shown in Figure 2. In Table 1 the characteristics of the as-manufactured composite materials are summarized.

**Table 1.** Characteristics of the as-manufactured hybrid composites.

Material ID	Matrix Type	Total Fiber Volume Fraction	Thickness (mm)
H_Ep	Thermoset-Epoxy	0.38 ± 0.02	2.0 ± 0.1
H_PP	Thermoplastic-PP	0.36 ± 0.02	2.1 ± 0.1
H_PPc	Thermoplastic-PPc	0.35 ± 0.03	2.2 ± 0.1

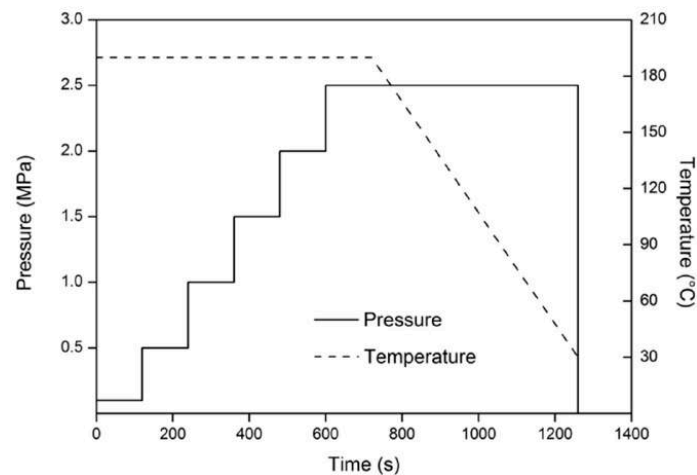


**Figure 2.** Processing conditions used to manufacture polypropylene (PP)- and polypropylene modified with a coupling agent (PPc)- based composites.

### 2.3. Mechanical Characterization of Composites

Specimens with dimensions  $125 \times 20 \times t$  ( $l \times w \times t$ ) were subjected to three-point bending tests in accordance with ASTM D790 (West Conshohocken, PA, USA) with a support span-to-thickness ratio of 32:1 and a cross-head speed of 5 mm/min and 2.5 mm/min for thermoplastic and thermoset-based composites, respectively. Tests were carried out on a Zwick/Roell Z010 universal testing machine (Ulm, Germany) equipped with a 10 kN load cell. The flexural strain was measured by a sensor arm for flexure test that was connected with an automatic extensometer. Specimens were tested in two orientations: with flax fibers along the longitudinal direction (warp fiber direction,  $F_L$ ) and with basalt fibers along the longitudinal direction (weft fiber direction,  $B_L$ ). Five specimens were tested for each configuration and matrix type.

Test coupons measuring  $100 \times 100$  mm were impacted at room temperature at target kinetic impact energies ranging from 5 J to 30 J. An instrumented drop-weight impact testing machine (Instron/CEAST 9340, Pianezza, Italy) was used to this purpose equipped with a hemispherical tip (diameter of 12.7 mm). Three specimens for each matrix type and energy level were impacted out-of-plane with a constant mass of 8.055 kg while being clamped between two steel plates with a circular unsupported area of 40 mm (diameter). The force–time curves were recorded during each test by the DAS64K acquisition system.

### 2.4. Morphological and Damage Investigation

The fracture surfaces of specimens which failed in bending were investigated by scanning electron microscopy (FE-SEM MIRA3 by TESCAN, Brno, Czech Republic). All specimens were sputter coated with gold prior to FE-SEM observations.

The dent depth of each impacted coupon was measured using a laser profilometer (Taylor–Hobson Talyscan 150) with a scanning speed of 8500  $\mu\text{m/s}$ . The scanned images were processed with the analysis software TalyMap 3D.

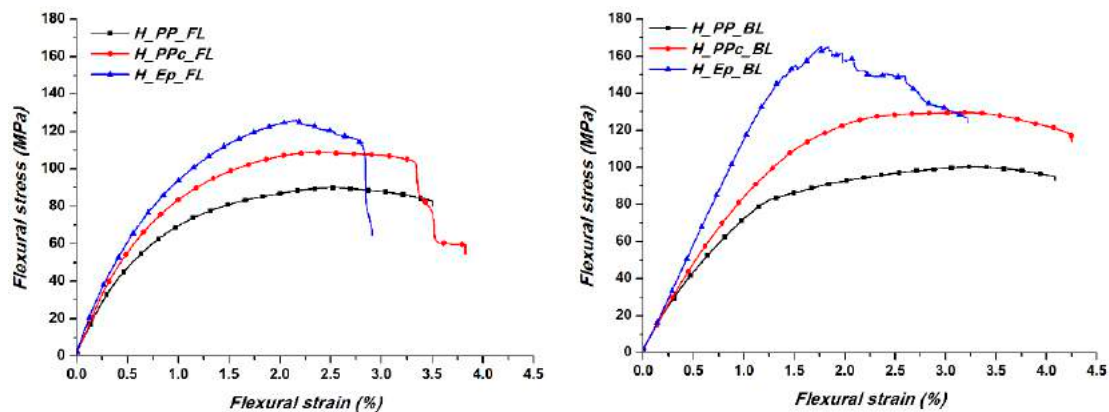
## 3. Results and Discussion

### 3.1. Quasi-Static Flexural Behaviour

The flexural properties are summarized in Table 2, while Figure 3 shows representative stress–strain curves obtained at room temperature.

**Table 2.** Summary of flexural properties of flax/basalt hybrid laminates.

Specimen ID	Flexural Strength (MPa)	Flexural Modulus (GPa)	Strain at Maximum Stress (%)
H_PP_FL	85.9 ± 3.9	10.5 ± 0.4	2.6 ± 0.3
H_PP_BL	101.0 ± 0.9	9.5 ± 0.1	3.2 ± 0.1
H_PPc_FL	106.8 ± 2.3	12.6 ± 0.4	2.5 ± 0.3
H_PPc_BL	129.3 ± 1.8	9.9 ± 0.4	3.2 ± 0.6
H_Ep_FL	128.6 ± 4.8	14.4 ± 0.4	2.4 ± 0.2
H_Ep_BL	165.2 ± 5.4	11.2 ± 0.2	1.8 ± 0.2

**Figure 3.** Typical stress vs. strain curves for flax/basalt composites along the warp (FL) and weft (BL) fiber directions.

For both matrices, a difference in the flexural modulus can be highlighted between warp and weft directions, which is likely to be ascribed to the higher fiber volume fraction of flax fibers in specimens when tested with flax fibers oriented in the longitudinal direction. As expected, composites with a thermoplastic matrix exhibited a much more ductile behavior compared to the epoxy resin. The ductility of PP was able to partially relieve the stress concentrations created in the matrix by defects (kink bands) always present in flax fibers [29]. This explanation supports the higher ductility observed in specimens tested along the basalt fibers, which are not characterized by such defects. Specimens tested with basalt fibers aligned along the longitudinal direction showed the highest flexural strength irrespective of the matrix type, which is due to the better absolute mechanical properties of basalt fibers compared to flax fibers. Usually flax fiber reinforced composites are characterized by a sudden failure due to the poor strain at failure of flax fibers (~1.2–1.8%) [30,31], while in the present case the hybridization with much more ductile basalt fibers [32] allowed the composites to fail in a much more gradual manner, especially when tested with basalt fibers in the longitudinal direction.

All the curves exhibited a significant non-linear behavior at low strains, which needs to be ascribed to the presence of flax fibers and seems only to be emphasized by the ductile PP. Many authors have pointed out this behavior [33,34] that seems to represent a peculiarity of natural fibers, as it has been reported to occur not only in flax [35,36] but also in wood [37] and hemp [38]. Recent studies tried to provide explanations for this behavior, and several mechanisms have been proposed, including cellulose microfibrils reorientation, shear strain-induced crystallization of the amorphous paracrystalline components and degree of ellipticity of the fiber's cross-section [38,39]. Indeed, this effect is significantly reduced in epoxy-based laminates when tested with basalt fibers in the longitudinal direction.

The presence of a coupling agent in the PP matrix caused an increase in both the flexural strength and modulus, without affecting in a significant way the ductility of the resulting composites. These results are due to the improvement of fiber/matrix interfacial adhesion for both fiber types. It is well known that the interactions between the anhydride groups of maleated coupling agents and the

hydroxyl groups of flax and basalt fibers through esterification reactions can alleviate fiber/matrix incompatibility issues [40,41].

The fiber/matrix adhesion has been investigated by scanning electron microscopy. The level of interfacial adhesion of flax and basalt fibers with neat PP was found to be nonoptimal, as can be seen in Figure 4, where pull-out (Figure 4a,c,f) and debonding (Figure 4b,d,e) represent the dominant failure modes. In Figure 5 it is possible to note that both fibers, flax and basalt, benefited from the addition of the coupling agent. The pull-out was significantly reduced, and the fibers appear to be covered with a layer of polymer matrix, with ligaments connecting the fibers to the matrix (Figure 5a,b,d–f). For comparison purposes, the surface of pristine flax and basalt fibers is included in Figure 5g,h, respectively.

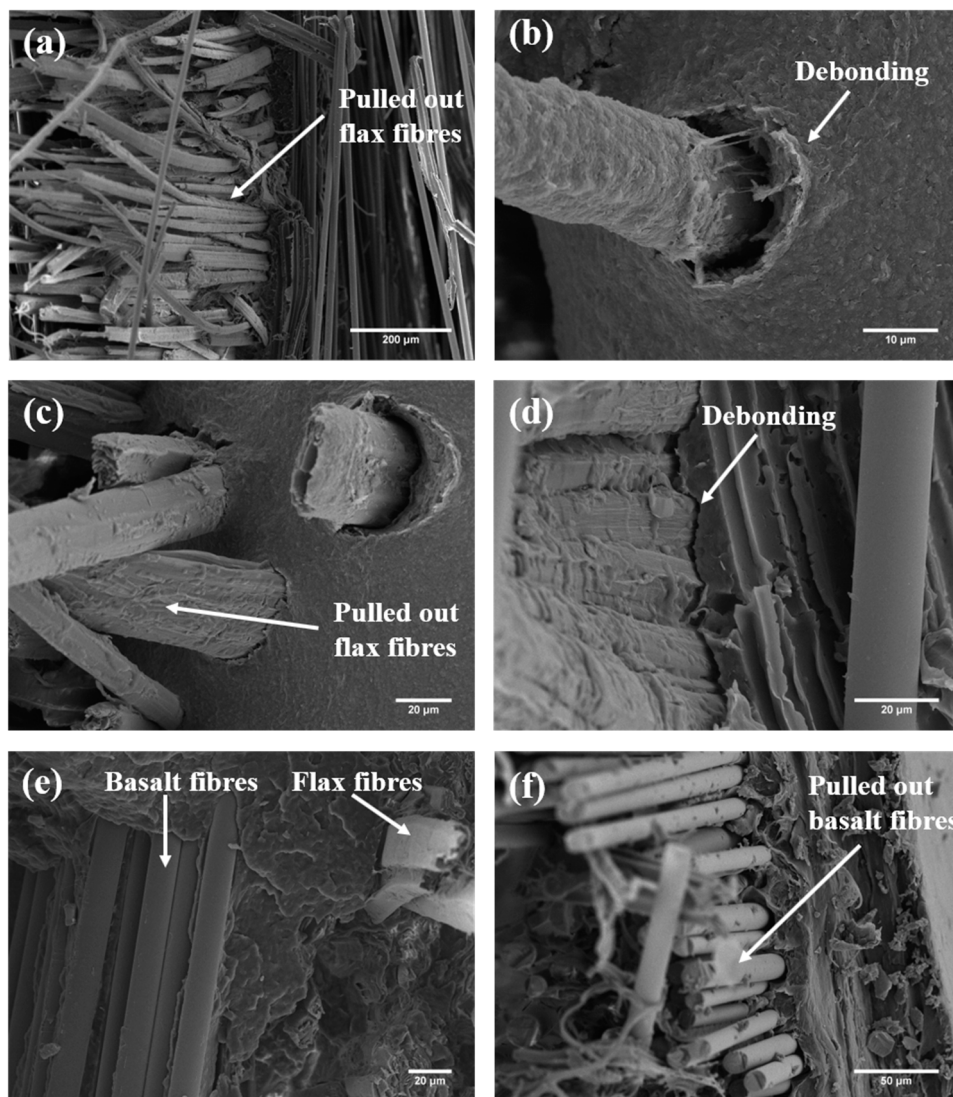


**Figure 4.** SEM micrographs of failed flexural H\_PP specimens at different magnifications, highlighting the presence of extensive fiber pull-out (a,c,f) and fiber/matrix debonding (b,d,e).

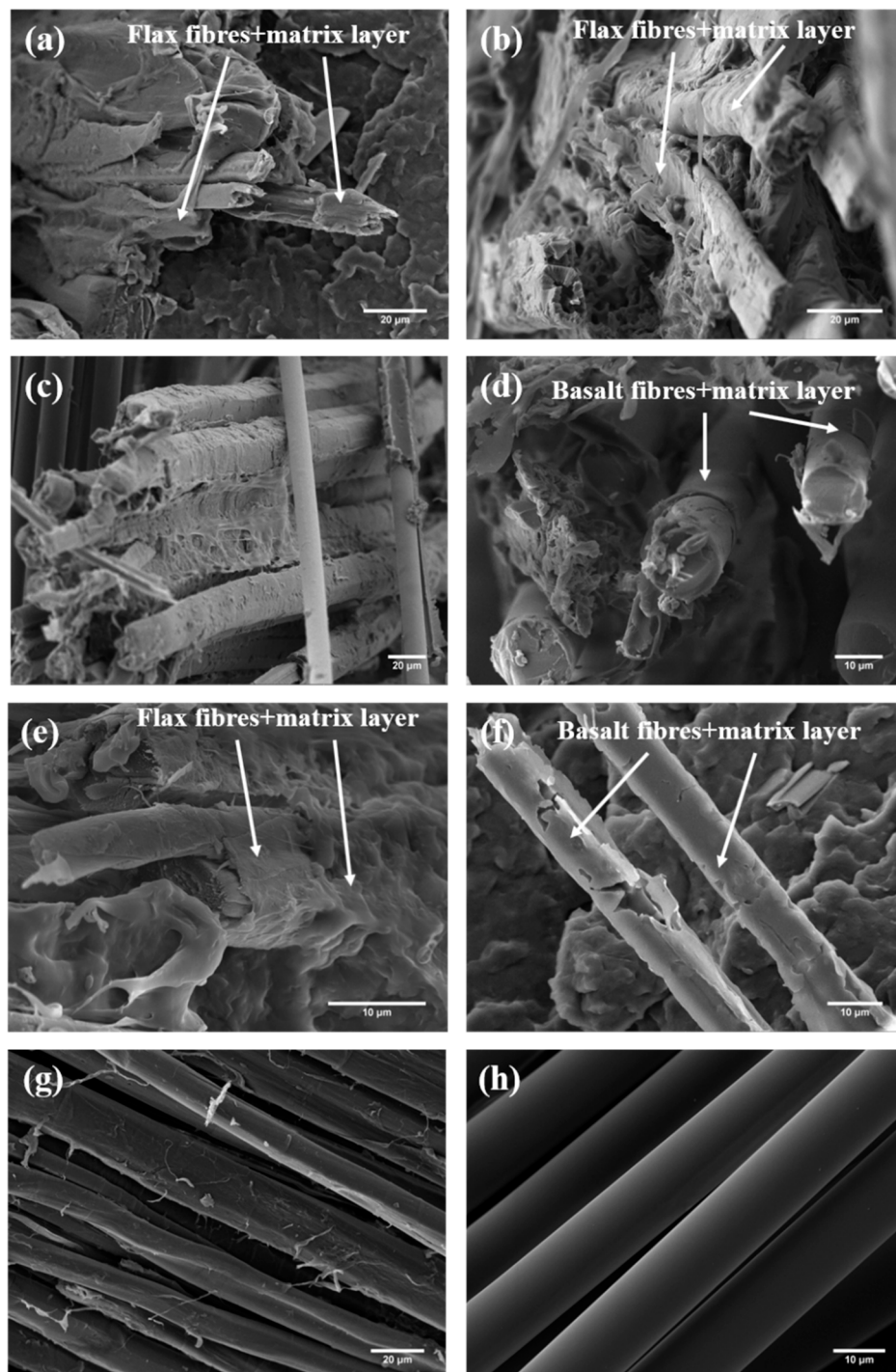


**Figure 5.** SEM micrographs of failed flexural H\_PPc specimens at different magnifications, highlighting the presence of matrix layers on basalt (c,d,f) and flax fibers (a,b,e). Micrographs (g) and (h) show pristine flax and basalt fibers as extracted from the fabric, respectively.

For epoxy-based composites, the fracture surface exhibited a “blocky” appearance (Figure 6a,b,d) especially with basalt fibers fractured on the same plane, while also flax fibers were characterized by a sufficient level of adhesion as it can be inferred from the extensive fiber fibrillation (Figure 6c) coupled with the presence of epoxy residues on the fiber surface (Figure 6d,f). This supports the good mechanical behavior exhibited by the biocomposites, when compared with results available in literature.

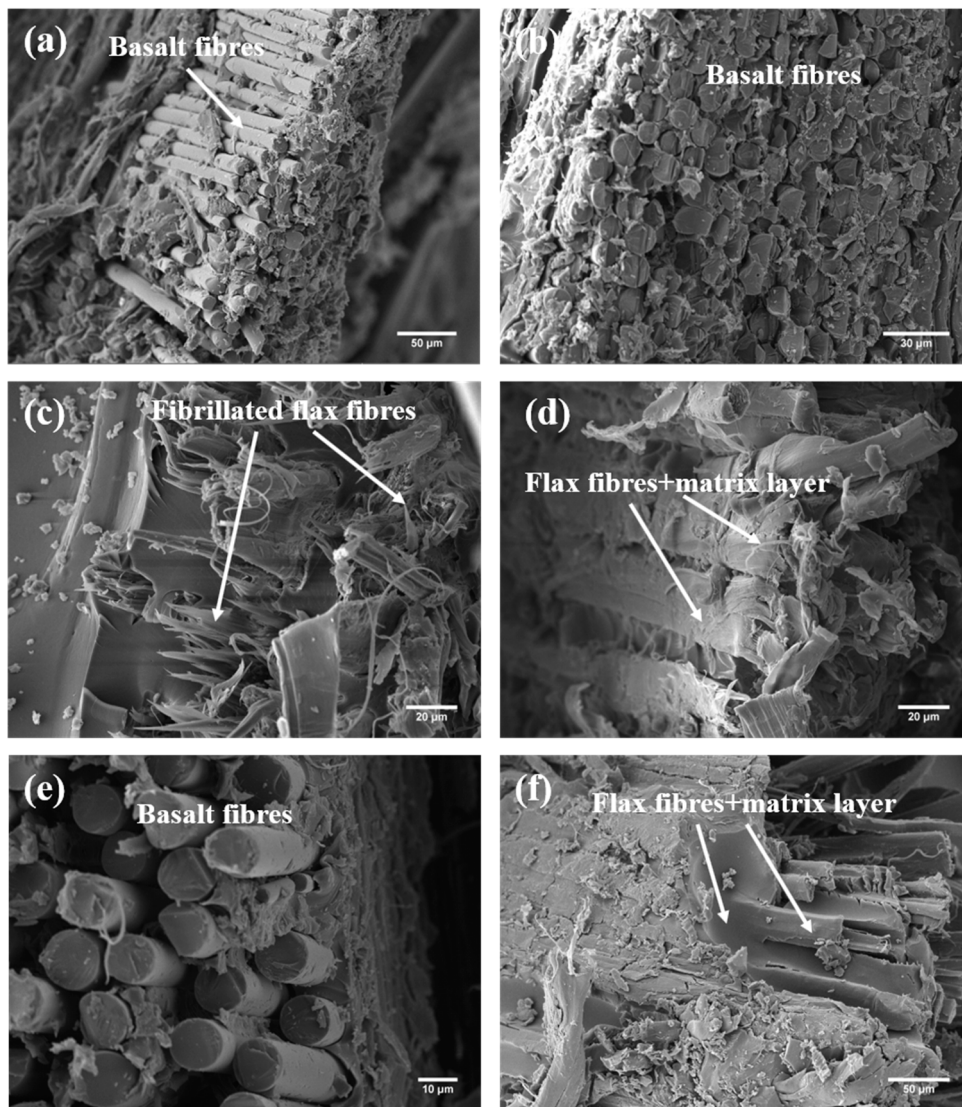


**Figure 6.** SEM micrographs of failed flexural H<sub>E</sub>p specimens at different magnifications, the presence of matrix layers on basalt (a,b,e) and flax fibers (d,f) and flax fiber fibrillation (c).

Despite the difficulties in comparing composites with different fiber volume fractions and fiber architectures, Meredith et al. [42] investigated several flax/epoxy composites based on the same weave style (Twill 2/2). The flexural strength was found to range from 57.0 to 195.2 MPa for fiber volume fractions from 37 to 54%, while flexural modulus was in the range 2.12–7.81 GPa. Goutianos et al. [43] compared different flax fiber architectures in a vinylester matrix for fiber volume fractions in the range of 29 to 35%. Composites showed flexural strengths ranging from 80 to 140 MPa and flexural moduli from 5 to 10 GPa. Cihan et al. [44] investigated the mechanical performance of woven flax/E-glass hybrid composites. For flax fiber reinforced composites, with a fiber volume fraction around 0.36, the tensile strength and stiffness were reported to be 86.43 MPa and 8.89 GPa, respectively, while Blanchard et al. [45] for a volume fraction of flax fibers equal to 0.37 in an epoxy matrix, found a flexural strength and stiffness of 114.91 MPa and 6.13 GPa, respectively. In the present case, by adding around 13% by volume of basalt fibers, it is possible to increase the flexural strength and modulus of 43% and 83%, respectively. In particular, it is worth noting the increase in flexural stiffness that can be obtained with the present hybrid, which could represent an opportunity to introduce flax fibers in semi-structural applications.



### 3.2. Low-Velocity Impact Behaviour

The representative force vs displacement curves of the hybrid composites as a function of matrix type and impact energy are reported in Figure 7. Matrix effect was not significant at 5 J (Figure 7a) as all the samples exhibited similar hysteresis loops, but for a 10 J-impact event some differences can be highlighted. In particular, epoxy-based laminates showed a more drastic load drop (Figure 7b) followed by the unloading curve. This substantial load drop points toward a loss of elastic energy and the vulnerability to fiber breakage and subsequent perforation, which was indeed reached at 15 J for thermoset-based composites (Figure 7c).

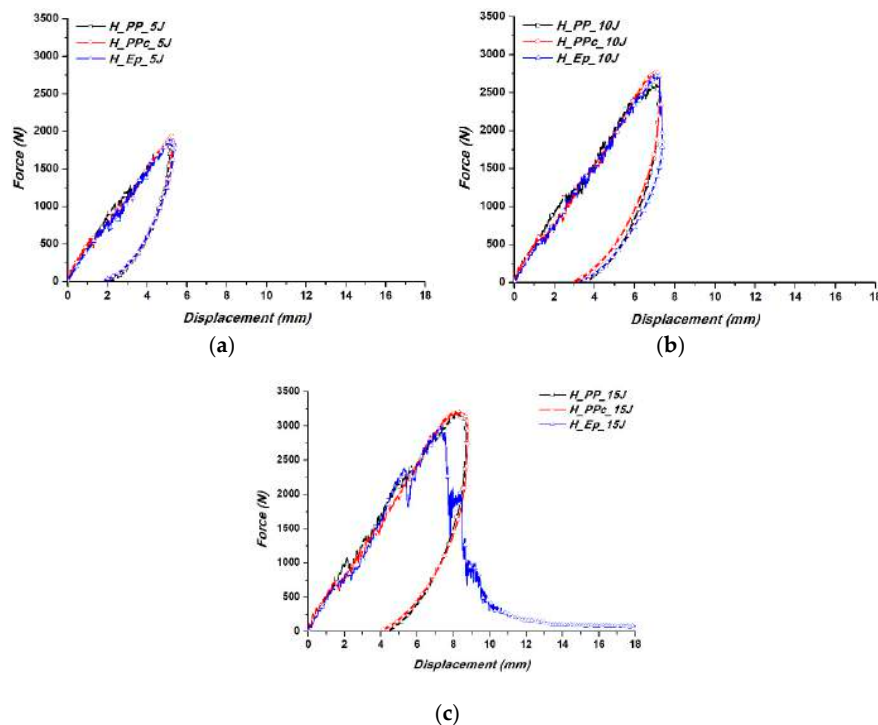


**Figure 7.** Typical force–displacement curves of flax/basalt hybrid composites at various impact energy levels: (a) 5 J; (b) 10 J, and (c) 15 J.

Epoxy laminates presented the lowest impact resistance at all impact energies, whereas thermoplastic-based laminates exhibited a very similar impact damage behavior in terms of force vs displacement response. The results compare quite favorably with those available in the literature for flax fiber reinforced epoxy composites. Bensadoun et al. [46] investigated the impact behavior of laminates with different flax fiber architectures and matrix types. Despite the unavoidable differences in impact parameters, similar conditions were used for laminates with a thickness of 2 mm and a total fiber volume fraction of 0.40. The authors found perforation energies ranging from 5.7 J to 7 J, which are lower than the value found in the present case (15 J).

It is suggested that basalt fiber hybridization in intraply configuration can improve the common poor impact response reported in the literature of plant fiber composites. The shift from a thermoset to a thermoplastic matrix markedly influenced the absorbed energy, as it can be clearly observed in Figure 8, where 30 J and 20 J were absorbed at perforation by PP- and PPc-based laminates, respectively.

In perforation impact tests, the fibers need to be broken to achieve perforation. Therefore, the stronger and tougher the fibers, the more pronounced is the role played by the fiber fracture energy in the total perforation energy. In the present case, as the fibers are the same for all the laminates, the relative contribution of the matrix ductility to the composite impact behavior is more important. Hybrid epoxy composites, at each impact energy, showed the highest damage degree, i.e., the ratio of absorbed energy to the kinetic impact energy, while the energy dissipated during impact is almost the

same in thermoplastic-based laminates at least up to 15 J. This ratio increases up to a maximum value of unity when perforation occurs.

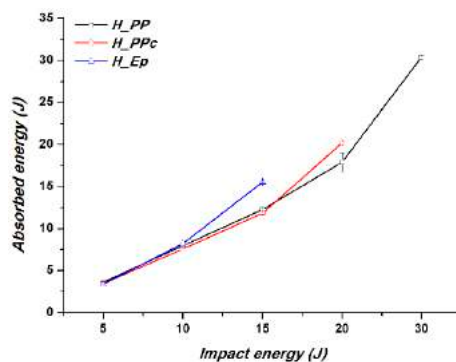


Figure 8. Impact energy vs. absorbed energy curves at various impact energy levels and matrix type.

The higher ductility of the PP matrix allows more energy absorption through plastic deformation compared to the brittle epoxy matrix, as observed by other authors [25,46]. This is supported by the assessment of the residual indentation depth, also known as dent depth, which has been performed by laser profilometry after impact (Figure 9).

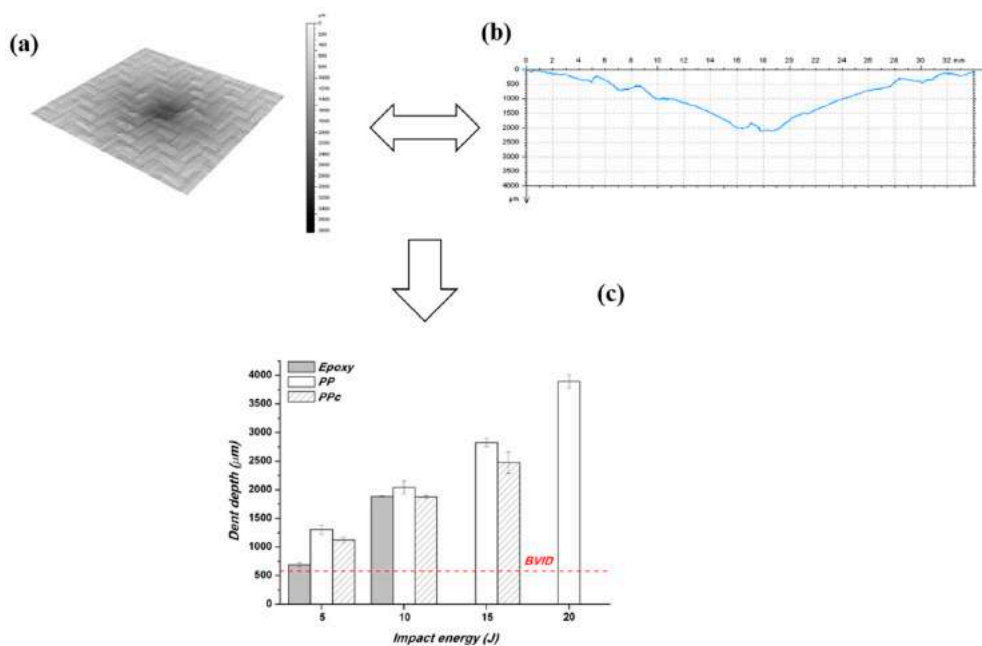
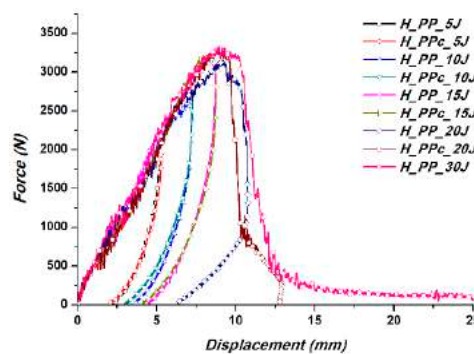


Figure 9. Dent depth: (a) 3-D image of damaged specimen; (b) extracted profile and (c) changes in dent depth on the impacted face of specimens as a function of impact energy and matrix type.

This type of damage can involve local matrix failure, local matrix plastic deformation, and local fiber breakage. At all impact energies, composites based on neat polypropylene exhibited a higher residual plastic deformation. It is also worth noting that, in accordance with the commonly accepted definition of BVID (Barely Visible Impact Damage) [25], the threshold of 0.6 mm (highlighted in Figure 9) is reached for all composites already at 5 J.

To better appreciate differences between compatibilized and neat polypropylene matrices, the representative force vs displacement curves for the whole range of impact energies are given in Figure 10. The effect of matrix type becomes significant with increasing impact energy (>15 J) (Figure 10). At 20 J, a more drastic load drop was exhibited by the compatibilized PP, while an

energy of 30 J was needed to perforate the specimens based on neat PP, likely due to different damage absorption mechanisms associated with the different extent of fiber/matrix adhesion.



**Figure 10.** Typical force–displacement curves of flax/basalt hybrid thermoplastic composites in the whole range of impact energies.

Macroscopic observation of the impacted specimens corroborates these results (Figures 11–13). The scale in each photograph has been adapted to highlight the different damage mechanisms. Thermoset composites exhibited a sharp failure pattern, typical of their brittle character (Figure 11), with the presence of cracks along warp/weft directions in the impacted side already for an impact energy level as low as 5 J. The intraply hybridization prevented the samples from exhibiting the characteristic diamond-shaped fracture surface on the rear side [15,25,46], which was characterized by fiber splitting and cracks mainly along the weft direction. It is interesting to note that these cracks run parallel to the basalt yarns and caused the failure only of the weaker flax yarns. After perforation at 15 J, a limited fiber pull-out was detected, thus, confirming the sufficient level of fiber/matrix adhesion.

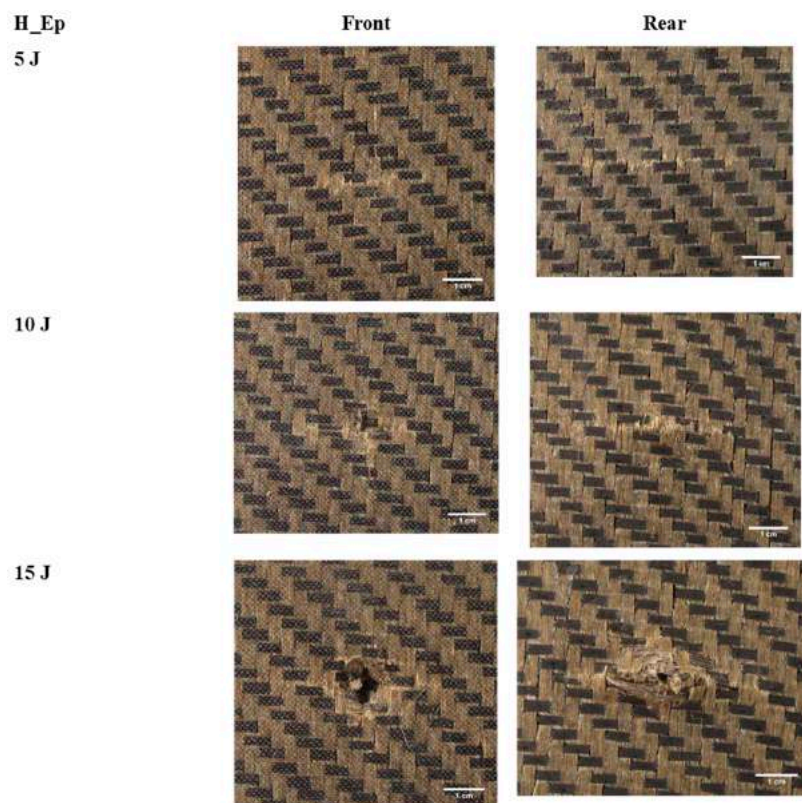


**Figure 11.** Close-up view of impact damage progression on front and rear surfaces of epoxy-based impacted specimens.

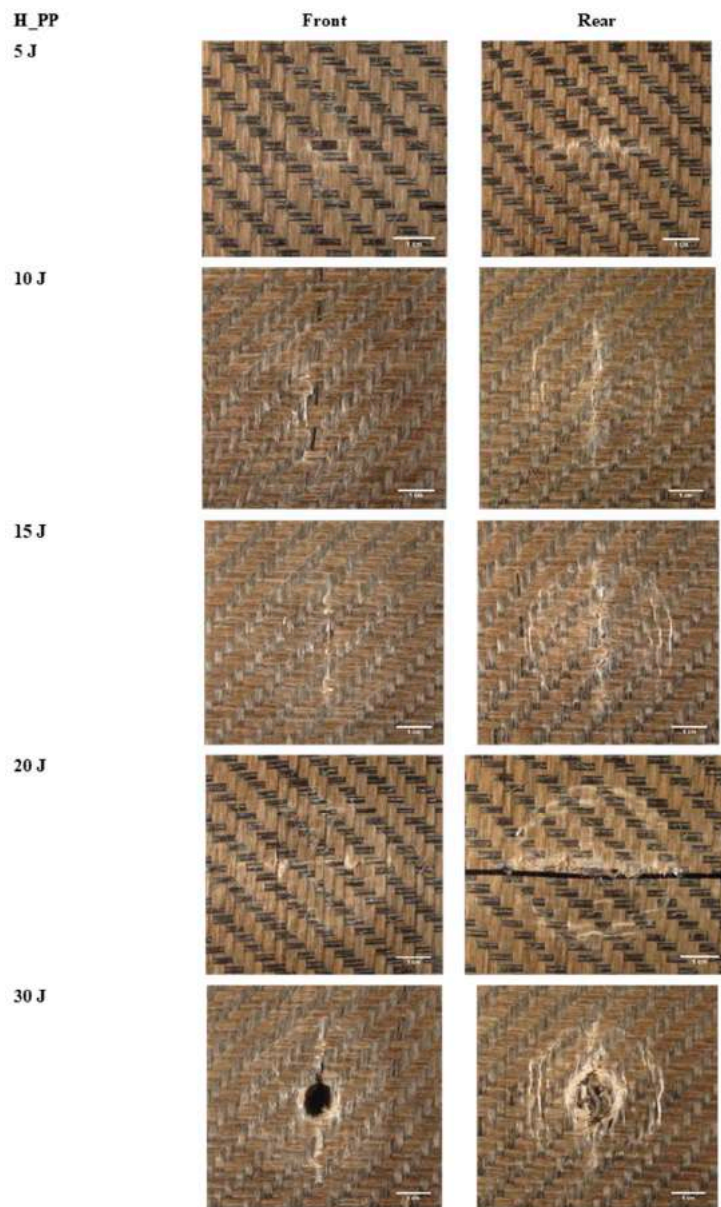


**Figure 12.** Close-up view of impact damage progression on front and rear surfaces of PP-based impacted specimens.

Thermoplastic-based laminates showed a different behavior, with a more ductile response to impact loading. In both cases (Figures 12 and 13) an extensive plastic deformation and a wider damaged area can be easily observed with the presence of matrix cracks and flax fiber failures on the impacted side.

A significant difference between compatibilized and neat PP is represented by the extensive stress whitening that occurred in all compatibilized samples (Figure 13). This phenomenon increased with increasing impact energy and extended up to the edges of the impacted plates. This can be related to the better fiber/matrix interfacial adhesion induced by the coupling agent that hindered the plastic deformation of the matrix, thus, forcing a larger amount of the sample to respond to the impact loading. This behavior was not observed in neat PP-based composites where the matrix was free to plastically deform under the contact point with the impactor, thus, causing a deeper indentation (Figure 9) and a higher energy absorption (Figure 8).

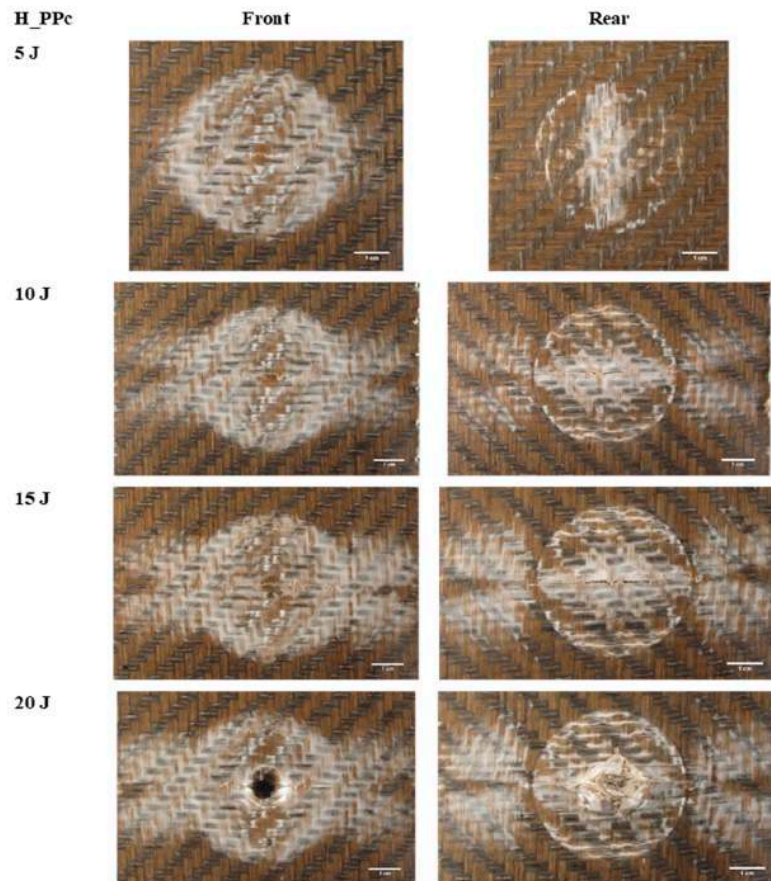


**Figure 13.** Close-up view of impact damage progression on front and rear surfaces of PPc-based impacted specimens.

It is worth mentioning that no necking and/or wrinkling were detected as damage mechanisms in polypropylene-based composites, which need to be avoided as they absorb additional energy compared to properly tested samples, as usually found in self-reinforced polypropylene composites if tested with small geometry ratios, i.e., the ratio of the sample size divided by the clamp size [47].

The higher bending strength of the PPc-based laminates combined with the higher strain at break of the thermoplastic compared to the thermoset matrix delayed the onset of first damage because plastic deformation occurred before the matrix failure, thus, ensuring a higher peak force under impact, which represents the maximum load a laminate can tolerate before major damage (Figure 14).

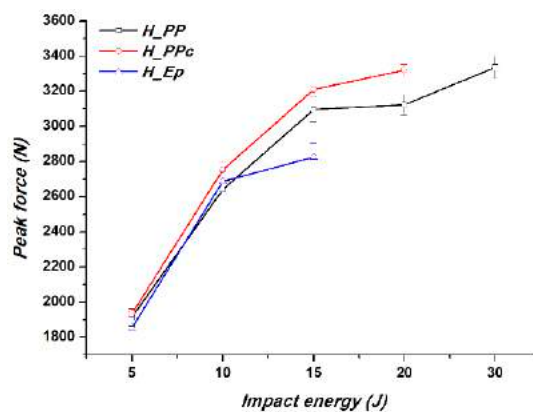


**Figure 14.** Peak force vs kinetic impact energy for flax/basalt hybrid composites as a function of matrix type.

#### 4. Conclusions

A new intraply hybrid composite using basalt and flax fibers has been manufactured and tested in both quasi-static (three-point bending) and dynamic (low-velocity impact) conditions with the main aim of assessing the effect of matrix behavior. In this regard, three different matrices have been investigated, namely epoxy, polypropylene, and a polypropylene compatibilized with maleic anhydride. The matrix ductility was found to have a significant influence on the impact response only at energies higher than 5 J, while composites based on compatibilized PP showed the best combination of properties in terms of quasi-static strength, energy absorption, peak force, and perforation energy.

Basalt fiber hybridization in intraply configuration significantly improved the common poor impact response of plant fiber composites usually reported in the literature, preventing the growth of cracks in a diamond-shaped pattern and balancing the poor transverse strength of flax fibers. Thermoplastic-based laminates exhibited a concentrated (circular) damaged zone at perforation due to the extensive plastic deformation that hindered further extension of the cross-shaped cracks, thus, enhancing the energy absorption of the resulting hybrid laminates. For 2-mm thick hybrid laminates, perforation threshold was found to lie in the range of 20 to 30 J, depending on the presence or not of the coupling agent, respectively. The results confirm the suitability of polypropylene-based intraply hybrid composites to impact-related applications.

**Author Contributions:** Conceptualization, F.S., J.T., C.S. and P.R.; methodology, F.S. and L.F.; formal analysis, F.S., J.T. and C.S.; investigation, L.F., G.S., F.C., M.R.R. and V.A.; writing—original draft preparation, F.S.; writing—review and editing, F.S., P.R., M.R.R., V.A. and J.T.; supervision, F.S. and J.T.

**Funding:** This research received no external funding.

**Conflicts of Interest:** The authors declare no conflict of interest.

#### References

1. Swolfs, Y.; Verpoest, I.; Gorbatiikh, L. Recent advances in fibre-hybrid composites: Materials selection, opportunities and applications. *Int. Mater. Rev.* **2018**, *1*–35. [[CrossRef](#)]
2. Swolfs, Y.; Gorbatiikh, L.; Verpoest, I. Fibre hybridisation in polymer composites: A review. *Compos. Part A Appl. Sci. Manuf.* **2014**, *67*, 181–200. [[CrossRef](#)]
3. Manders, P.W.; Bader, M.G. The strength of hybrid glass/carbon fibre composites. *J. Mater. Sci.* **1981**, *16*, 2233–2245. [[CrossRef](#)]
4. Safri, S.N.A.; Sultan, M.T.H.; Jawaid, M.; Jayakrishna, K. Impact behaviour of hybrid composites for structural applications: A review. *Compos. Part B Eng.* **2018**, *133*, 112–121. [[CrossRef](#)]
5. Naik, N.; Ramasimha, R.; Arya, H.; Prabhu, S.; ShamaRao, N. Impact response and damage tolerance characteristics of glass–carbon/epoxy hybrid composite plates. *Compos. Part B Eng.* **2001**, *32*, 565–574. [[CrossRef](#)]
6. Hosur, M.V.; Adbullah, M.; Jeelani, S. Studies on the low-velocity impact response of woven hybrid composites. *Compos. Struct.* **2005**, *67*, 253–262. [[CrossRef](#)]
7. Sayer, M.; Bektaş, N.B.; Sayman, O. An experimental investigation on the impact behavior of hybrid composite plates. *Compos. Struct.* **2010**, *92*, 1256–1262. [[CrossRef](#)]
8. Gustin, J.; Joneson, A.; Mahinfalah, M.; Stone, J. Low velocity impact of combination Kevlar/carbon fiber sandwich composites. *Compos. Struct.* **2005**, *69*, 396–406. [[CrossRef](#)]
9. Salehi-Khojin, A.; Mahinfalah, M.; Bashirzadeh, R.; Freeman, B. Temperature effects on Kevlar/hybrid and carbon fiber composite sandwiches under impact loading. *Compos. Struct.* **2007**, *78*, 197–206. [[CrossRef](#)]
10. Wan, Y.Z.; Wang, Y.L.; He, F.; Huang, Y.; Jiang, H.J. Mechanical performance of hybrid bismaleimide composites reinforced with three-dimensional braided carbon and Kevlar fabrics. *Compos. Part A Appl. Sci. Manuf.* **2007**, *38*, 495–504. [[CrossRef](#)]
11. Imielińska, K.; Castaings, M.; Wojtyra, R.; Haras, J.; Le Clezio, E.; Hosten, B. Air-coupled ultrasonic C-scan technique in impact response testing of carbon fibre and hybrid: Glass, carbon and Kevlar/epoxy composites. *J. Mater. Process. Technol.* **2004**, *157–158*, 513–522. [[CrossRef](#)]

12. Ying, S.; Mengyun, T.; Zhijun, R.; Baohui, S.; Li, C. An experimental investigation on the low-velocity impact response of carbon–aramid/epoxy hybrid composite laminates. *J. Reinf. Plast. Compos.* **2017**, *36*, 422–434. [[CrossRef](#)]
13. Petrucci, R.; Santulli, C.; Puglia, D.; Nisini, E.; Sarasini, F.; Tirillò, J.; Torre, L.; Minak, G.; Kenny, J.M. Impact and post-impact damage characterisation of hybrid composite laminates based on basalt fibres in combination with flax, hemp and glass fibres manufactured by vacuum infusion. *Compos. Part B Eng.* **2015**, *69*, 507–515. [[CrossRef](#)]
14. Ahmed, K.S.; Vijayarangan, S.; Kumar, A. Low Velocity Impact Damage Characterization of Woven Jute Glass Fabric Reinforced Isothalic Polyester Hybrid Composites. *J. Reinf. Plast. Compos.* **2007**, *26*, 959–976. [[CrossRef](#)]
15. Sarasini, F.; Tirillò, J.; D’Altilia, S.; Valente, T.; Santulli, C.; Touchard, F.; Chocinski-Arnault, L.; Mellier, D.; Lampani, L.; Gaudenzi, P. Damage tolerance of carbon/flax hybrid composites subjected to low velocity impact. *Compos. Part B Eng.* **2016**, *91*, 144–153. [[CrossRef](#)]
16. Al-Hajaj, Z.; Sy, B.L.; Bougherara, H.; Zdero, R. Impact properties of a new hybrid composite material made from woven carbon fibres plus flax fibres in an epoxy matrix. *Compos. Struct.* **2019**, *208*, 346–356. [[CrossRef](#)]
17. Förster, T.; Hao, B.; Mäder, E.; Simon, F.; Wölfel, E.; Ma, P.-C.; Förster, T.; Hao, B.; Mäder, E.; Simon, F.; et al. CVD-Grown CNTs on Basalt Fiber Surfaces for Multifunctional Composite Interphases. *Fibers* **2016**, *4*, 28. [[CrossRef](#)]
18. Fragassa, C.; Pavlovic, A.; Santulli, C. Mechanical and impact characterisation of flax and basalt fibre vinylester composites and their hybrids. *Compos. Part B Eng.* **2018**, *137*, 247–259. [[CrossRef](#)]
19. Dhakal, H.N.; Sarasini, F.; Santulli, C.; Tirillò, J.; Zhang, Z.; Arumugam, V. Effect of basalt fibre hybridisation on post-impact mechanical behaviour of hemp fibre reinforced composites. *Compos. Part A Appl. Sci. Manuf.* **2015**, *75*, 54–67. [[CrossRef](#)]
20. Papa, I.; Ricciardi, M.R.; Antonucci, V.; Pagliarulo, V.; Lopresto, V. Impact behaviour of hybrid basalt/flax twill laminates. *Compos. Part B Eng.* **2018**, *153*, 17–25. [[CrossRef](#)]
21. Pegoretti, A.; Fabbri, E.; Migliaresi, C.; Pilati, F. Intraply and interply hybrid composites based on E-glass and poly(vinyl alcohol) woven fabrics: Tensile and impact properties. *Polym. Int.* **2004**, *53*, 1290–1297. [[CrossRef](#)]
22. Wang, X.; Hu, B.; Feng, Y.; Liang, F.; Mo, J.; Xiong, J.; Qiu, Y. Low velocity impact properties of 3D woven basalt/aramid hybrid composites. *Compos. Sci. Technol.* **2008**, *68*, 444–450. [[CrossRef](#)]
23. Zhang, C.; Rao, Y.; Li, Z.; Li, W. Low-Velocity Impact Behavior of Interlayer/Intralayer Hybrid Composites Based on Carbon and Glass Non-Crimp Fabric. *Materials* **2018**, *11*, 2472. [[CrossRef](#)] [[PubMed](#)]
24. Bandaru, A.K.; Patel, S.; Sachan, Y.; Alagirusamy, R.; Bhatnagar, N.; Ahmad, S. Low velocity impact response of 3D angle-interlock Kevlar/basalt reinforced polypropylene composites. *Mater. Des.* **2016**, *105*, 323–332. [[CrossRef](#)]
25. Vieille, B.; Casado, V.M.; Bouvet, C. About the impact behavior of woven-ply carbon fiber-reinforced thermoplastic- and thermosetting-composites: A comparative study. *Compos. Struct.* **2013**, *101*, 9–21. [[CrossRef](#)]
26. Arikan, V.; Sayman, O. Comparative study on repeated impact response of E-glass fiber reinforced polypropylene & epoxy matrix composites. *Compos. Part B Eng.* **2015**, *83*, 1–6.
27. Mutjé, P.; Vallejos, M.E.; Gironès, J.; Vilaseca, F.; López, A.; López, J.P.; Méndez, J.A. Effect of maleated polypropylene as coupling agent for polypropylene composites reinforced with hemp strands. *J. Appl. Polym. Sci.* **2006**, *102*, 833–840. [[CrossRef](#)]
28. Mohanty, A.; Misra, M.; Hinrichsen, G. Biofibres, biodegradable polymers and biocomposites: An overview. *Macromol. Mater. Eng.* **2000**, *276–277*, 1–24. [[CrossRef](#)]
29. Hughes, M.; Carpenter, J.; Hill, C. Deformation and fracture behaviour of flax fibre reinforced thermosetting polymer matrix composites. *J. Mater. Sci.* **2007**, *42*, 2499–2511. [[CrossRef](#)]
30. Audibert, C.; Andreani, A.-S.; Lainé, É.; Grandidier, J.-C. Mechanical characterization and damage mechanism of a new flax-Kevlar hybrid/epoxy composite. *Compos. Struct.* **2018**, *195*, 126–135. [[CrossRef](#)]
31. Wambua, P.; Ivens, J.; Verpoest, I. Natural fibres: Can they replace glass in fibre reinforced plastics? *Compos. Sci. Technol.* **2003**, *63*, 1259–1264. [[CrossRef](#)]
32. Fiore, V.; Scalici, T.; Di Bella, G.; Valenza, A. A review on basalt fibre and its composites. *Compos. Part B Eng.* **2015**, *74*, 74–94. [[CrossRef](#)]

33. Poilane, C.; Cherif, Z.E.; Richard, F.; Vivet, A.; Ben Doudou, B.; Chen, J. Polymer reinforced by flax fibres as a viscoelastoplastic material. *Compos. Struct.* **2014**, *112*, 100–112. [[CrossRef](#)]
34. Hughes, M.; Hill, C.A.S.; Hague, J.R.B. The fracture toughness of bast fibre reinforced polyester composites Part 1 Evaluation and analysis. *J. Mater. Sci.* **2002**, *37*, 4669–4676. [[CrossRef](#)]
35. Baley, C. Analysis of the flax fibres tensile behaviour and analysis of the tensile stiffness increase. *Compos. Part A Appl. Sci. Manuf.* **2002**, *33*, 939–948. [[CrossRef](#)]
36. Mahboob, Z.; El Sawi, I.; Zdero, R.; Fawaz, Z.; Bougherara, H. Tensile and compressive damaged response in Flax fibre reinforced epoxy composites. *Compos. Part A Appl. Sci. Manuf.* **2017**, *92*, 118–133. [[CrossRef](#)]
37. Navi, P.; Rastogi, P.; Gresse, V.; Tolou, A. Micromechanics of wood subjected to axial tension. *Wood Sci. Technol.* **1995**, *29*, 411–429. [[CrossRef](#)]
38. Placet, V.; Cissé, O.; Lamine Boubakar, M. Nonlinear tensile behaviour of elementary hemp fibres. Part I: Investigation of the possible origins using repeated progressive loading with in situ microscopic observations. *Compos. Part A Appl. Sci. Manuf.* **2014**, *56*, 319–327. [[CrossRef](#)]
39. Del Mastro, A.; Trivaudey, F.; Guicheret-Retel, V.; Placet, V.; Boubakar, L. Nonlinear tensile behaviour of elementary hemp fibres: A numerical investigation of the relationships between 3D geometry and tensile behaviour. *J. Mater. Sci.* **2017**, *52*, 6591–6610. [[CrossRef](#)]
40. Keener, T.; Stuart, R.; Brown, T. Maleated coupling agents for natural fibre composites. *Compos. Part A Appl. Sci. Manuf.* **2004**, *35*, 357–362. [[CrossRef](#)]
41. Matuana, L.M.; Balatinecz, J.J.; Sodhi, R.N.S.; Park, C.B. Surface characterization of esterified cellulosic fibers by XPS and FTIR Spectroscopy. *Wood Sci. Technol.* **2001**, *35*, 191–201. [[CrossRef](#)]
42. Meredith, J.; Coles, S.R.; Powe, R.; Collings, E.; Cozien-Cazuc, S.; Weager, B.; Müssig, J.; Kirwan, K. On the static and dynamic properties of flax and Cordenka epoxy composites. *Compos. Sci. Technol.* **2013**, *80*, 31–38. [[CrossRef](#)]
43. Goutianos, S.; Peijs, T.; Nystrom, B.; Skrifvars, M. Development of Flax Fibre based Textile Reinforcements for Composite Applications. *Appl. Compos. Mater.* **2006**, *13*, 199–215. [[CrossRef](#)]
44. Cihan, M.; Sobey, A.J.; Blake, J.I.R. Mechanical and dynamic performance of woven flax/E-glass hybrid composites. *Compos. Sci. Technol.* **2019**, *172*, 36–42. [[CrossRef](#)]
45. Blanchard, J.M.F.A.; Sobey, A.J.; Blake, J.I.R. Multi-scale investigation into the mechanical behaviour of flax in yarn, cloth and laminate form. *Compos. Part B Eng.* **2016**, *84*, 228–235. [[CrossRef](#)]
46. Bensadoun, F.; Depuydt, D.; Baets, J.; Verpoest, I.; van Vuure, A.W. Low velocity impact properties of flax composites. *Compos. Struct.* **2017**, *176*, 933–944. [[CrossRef](#)]
47. Meerten, Y.; Swolfs, Y.; Baets, J.; Gorbatikh, L.; Verpoest, I. Penetration impact testing of self-reinforced composites. *Compos. Part A Appl. Sci. Manuf.* **2015**, *68*, 289–295. [[CrossRef](#)]



© 2019 by the authors. Licensee MDPI, Basel, Switzerland. This article is an open access article distributed under the terms and conditions of the Creative Commons Attribution (CC BY) license (<http://creativecommons.org/licenses/by/4.0/>).